Synthesis, Structures, and Properties of Strained Spirocyclic [1]Sila- and [1]Germaferrocenophanes and Tetraferrocenylsilane

Mark J. MacLachlan,† Alan J. Lough,† William E. Geiger,*,‡ and Ian Manners*,†

Departments of Chemistry, University of Toronto, 80 St. George Street, Toronto M5S 3H6, Ontario, Canada, and University of Vermont, Burlington, Vermont 05405-0125

Received December 6, 1997

The spirocyclic [1]ferrocenophanes $[Fe(\eta\text{-}C_5H_4)_2]_2E$ (**3**, E = Si; **4**, E = Ge) and $Fe(\eta\text{-}C_5H_4)_2\text{-}Si(CH_2)_3$ (**5**) have been prepared by the reaction of $Fe(\eta\text{-}C_5H_4Li)_2\cdot$TMEDA (TMEDA = tetramethylethylenediamine) with $SiCl_4$, $GeCl_4$, and $Cl_2Si(CH_2)_3$, respectively. Single-crystal X-ray diffraction studies of **3**−**5** revealed that the molecules possess highly strained structures with tilt angles between the planes of the cyclopentadienyl rings of 19.4(2), 19.1(5), and 20.61(8)°, respectively. The Fe- - -Fe distances in **3** and **4** are 5.314(1) and 5.518(4) Å, and evidence for metal−metal interactions in the form of substantial redox coupling ($\Delta E_{1/2}$ = 0.37 V for **3** and 0.25 V for **4**) is present in the cyclic voltammograms of these species. For structural comparison, the tetraferrocenylsilane $[(\eta\text{-}C_5H_5)Fe(\eta\text{-}C_5H_4)]_4Si$ (**6**) was prepared and was characterized by single-crystal X-ray diffraction. Cyclic voltammetry of **6** showed four reversible oxidation waves with $E_{1/2}$ values of −0.03 to +0.39 V versus ferrocene; $\Delta E_{1/2}$ values of 0.10−0.18 V were indicative of significant metal−metal interactions. The results of Mössbauer, IR, and Raman studies of compounds **3**, **4**, and **6** are also discussed.

Introduction

The incorporation of transition metals into polymer backbones has been shown to generate materials with unusual physical and chemical properties.[1,2] In this regard, ferrocene represents an appealing structural unit to include in a polymer main chain, but, until recently, high-molecular-weight poly(metallocenes) have been very rare.[3−5] We have previously shown that strained silicon-bridged [1]ferrocenophanes such as **1a** undergo thermal ring-opening polymerization (ROP) to afford high-molecular-weight poly(ferrocenylsilanes) (e.g. **2a**).[5] Recently, anionic and transition-metal-catalyzed ring-opening polymerization have also been established as facile routes to these materials.[6] Ring-opened poly(metallocenes) are now known with a variety of bridging elements (for example, Ge as in **2b**), and studies have shown that these materials possess intriguing physical properties.[2,7−9] As cross-linking of poly(ferrocenes) is essential for many applications (e.g. for the formation of redox-active gels[10]), we targeted a convenient method of cross-linking materials such as **2a** which would be expected to lead to enhanced mechanical properties, thermal stability, and ceramic yields.

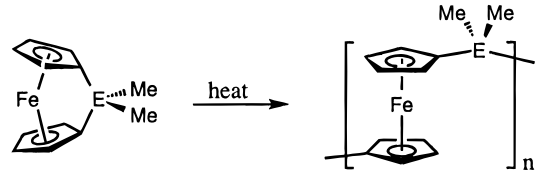

1a (E = Si) **2a** (E = Si)
1b (E = Ge) **2b** (E = Ge)

We identified the spirocyclic [1]ferrocenophanes **3** and **4** as possible cross-linking agents for poly(ferrocenes)

† University of Toronto.
‡ University of Vermont.

(1) For recent examples of transition-metal-based polymeric materials, see, for example: (a) Pittman, C. U.; Carraher, C. E.; Zeldin, M.; Sheats, J. E.; Culbertson, B. M., Eds. *Metal-Containing Polymeric Materials*; Plenum Press: New York, 1996. (b) Altman, M.; Bunz, U. H. F. *Angew. Chem., Int. Ed. Engl.* **1995**, *34*, 569. (c) Rosenblum, M.; Nugent, H. M.; Jang, K.-S.; Labes, M. M.; Cahalane, W.; Klemarczyk, P.; Reiff, W. M. *Macromolecules* **1995**, *28*, 6330. (d) Chen, H.; Archer, R. D. *Macromolecules* **1995**, *28*, 1609. (e) Stanton, C. E.; Lee, T. R.; Grubbs, R. H.; Lewis, N. S.; Pudelski, J. K.; Callstrom, M. R.; Erickson, M. S.; McLaughlin, M. L. *Macromolecules* **1995**, *28*, 8713. (f) Buretea, M. A.; Tilley, T. D. *Organometallics* **1997**, *16*, 1507. (g) Southard, G. E.; Curtis, M. D. *Organometallics* **1997**, *16*, 5618.

(2) Manners, I. *Angew. Chem., Int. Ed. Engl.* **1996**, *35*, 1602.

(3) (a) Brandt, P. F.; Rauchfuss, T. B. *J. Am. Chem. Soc.* **1992**, *114*, 1926. (b) Compton, D. L.; Brandt, P. F.; Rauchfuss, T. B.; Rosenbaum, D. F.; Zukoski, C. F. *Chem. Mater.* **1995**, *7*, 2342.

(4) Nugent, H. M.; Rosenblum, M.; Klemarczyk, P. *J. Am. Chem. Soc.* **1993**, *115*, 3848.

(5) Foucher, D. A.; Tang, B.-Z.; Manners, I. *J. Am. Chem. Soc.* **1992**, *114*, 6246.

(6) (a) Ni, Y.; Rulkens, R.; Manners, I. *J. Am. Chem. Soc.* **1996**, *118*, 4102. (b) Ni, Y.; Rulkens, R.; Pudelski, J. K.; Manners, I. *Macromol. Rapid Commun.* **1995**, *16*, 637. (c) Reddy, N. P.; Yamashita, H.; Tanaka, M. *J. Chem. Soc., Chem. Commun.* **1995**, 2263.

(7) Manners, I. *Adv. Organomet. Chem.* **1995**, *37*, 131.

(8) (a) Rulkens, R.; Resendes, R.; Verma, A.; Manners, I.; Murti, K.; Fossum, E.; Miller, P.; Matyjaszewski, K. *Macromolecules* **1997**, *30*, 8165. (b) Liu, X.-H.; Bruce, D. W.; Manners, I. *Chem. Commun.* **1997**, 289. (c) Pudelski, J. K.; Rulkens, R.; Foucher, D. A.; Lough, A. J.; Macdonald, P. M.; Manners, I. *Macromolecules* **1995**, *28*, 7301. (d) Pudelski, J. K.; Foucher, D. A.; Honeyman, C. H.; Macdonald, P. M.; Manners, I.; Barlow, S.; O'Hare, D. *Macromolecules* **1996**, *29*, 1894. (e) MacLachlan, M. J.; Aroca, P.; Coombs, N.; Manners, I.; Ozin, G. A. *Adv. Mater.* **1998**, *10*, 144.

(9) (a) Nguyen, M. T.; Diaz, A. F.; Dement'ev, V. V.; Pannell, K. H. *Chem. Mater.* **1993**, *5*, 1389. (b) Tanaka, M.; Hayashi, T. *Bull. Chem. Soc. Jpn.* **1993**, *66*, 334. (c) Barlow, S.; Rohl, A. L.; Shi, S.; Freeman, C. M.; O'Hare, D. *J. Am. Chem. Soc.* **1996**, *118*, 7578. (d) Hmyene, M.; Yassar, A.; Escorne, M.; Percheron-Guegan, A.; Garnier, F. *Adv. Mater.* **1994**, *6*, 564.

(10) Tatsuma, T.; Takada, K.; Matsui, H.; Oyama, N. *Macromolecules* **1994**, *27*, 6687.

S0276-7333(97)01071-6 CCC: $15.00
Publication on Web 04/11/1998

2a and **2b**, respectively. In addition, as silacyclobutanes

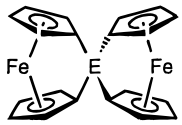

3 (E = Si)
4 (E = Ge)

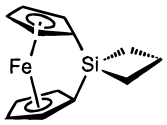

5

are also known to undergo thermal and transition-metal-catalyzed ROP, the novel spirocyclic [1]silaferrocenophane **5** incorporating a silacyclobutane group was also expected to function as a cross-linking agent. It is noteworthy that compounds such as **3**−**5** may also function as volatile precursors to novel composite materials.[8e] In this paper, we report full details on the synthesis, characterization, and properties of all three potential cross-linking agents (**3**−**5**). We also describe the synthesis and properties of tetraferrocenylsilane **6**, which provided useful comparative spectroscopic and structural data for **3**. Details of the polymerization behavior of **3** and **5** and the properties of the novel cross-linked poly(ferrocene) products, which were briefly described in a recent communication,[11] will be discussed in detail elsewhere.[12]

Results and Discussion

Synthesis of the Spirocyclic [1]Ferrocenophanes 3−5 and Tetraferrocenylsilane 6. In 1975, Osborne and Whiteley reported the synthesis of **3**, which was the first characterized spirocyclic [1]ferrocenophane.[13] These researchers isolated **3** in very low yield (7%) from the reaction of 2 equiv of dilithioferrocene·TMEDA ($fcLi_2$·TMEDA) with tetrachlorosilane, and the product was characterized by mass spectrometry, ^{1}H NMR, and UV−vis spectroscopy. In 1980, the same group reported further spectroscopic studies (Mössbauer, ^{13}C NMR) of the compound and a slight improvement in the yield (17%).[14] Interestingly, they attempted to determine the X-ray crystal structure of **3** but reported that the crystals obtained were disordered and not suitable for X-ray diffraction studies. The synthesis of the spirocyclic [1]germaferrocenophane **4** was also reported by Osborne and co-workers via an analogous route from $GeCl_4$.[15] This species was obtained in a low, unquantified yield and was characterized by mass spectrometry, NMR, and elemental analysis. The authors indicated that the isolation and purification of **4** were frustrated by decomposition in solution. Both compounds, **3** and **4**, have subsequently been investigated for protective derivatization of photoelectrochemical n-doped Si substrates.[16]

In our laboratory, **3** and **4** were synthesized using the same route as that described by Osborne and co-workers. However, the workup procedure was modified to improve the product yields. Filtration through a short column of alumina allowed any chlorinated silane/germane species and salts to be removed. The products isolated after the filtration were stable indefinitely in solution. The yield of **3** was improved significantly (70%), but the yield of **4** was still very low (<5%), probably due to a competition between Cp−Ge bond formation and anion-induced cleavage. Both **3** and **4** are air-stable red crystalline compounds. To allow additional comparison, we synthesized tetraferrocenylsilane **6** by the reaction of FcLi with $SiCl_4$ using a procedure analogous to that briefly described by Rosenberg in a patent.[17]

The spirocyclic species **3** and **4** were characterized by ^{1}H, ^{13}C, and ^{29}Si NMR, mass spectrometry, and IR, Raman, Mössbauer, and UV−vis spectroscopy. The ^{1}H NMR spectrum of **3** is interesting, as it displays a pair of pseudo-triplets in $CDCl_3$, as expected for an A_2B_2 spin system, but only a singlet in C_6D_6. When a sample of **3** in $CDCl_3$ was treated with a few drops of C_6D_6, the pseudo-triplets remained, confirming, as expected, that an unusual exchange mechanism was not reponsible for the magnetic equivalence of the protons. Since rotation of the Cp rings is impossible without ring-opening, there must be a fortuitous magnetic equivalence of the Cp protons in C_6D_6. This could be a consequence of unsymmetric proton shielding from the solvent. Due to steric crowding of the molecule, the β-protons are more accessible to solvent and may experience enhanced shielding from the aromatic ring of C_6D_6 relative to the α-protons. Exact compensation for the greater shielding usually observed for the Cp α-protons (closest to the Si substituent) would therefore arise. In contrast to **3**, the ^{1}H spectrum of the germanium analogue **4** is typical of a symmetric [1]ferrocenophane, with two pseudo-triplets in both C_6D_6 and $CDCl_3$. Compounds **3** and **4** display ^{13}C NMR spectra consistent with the assigned structures. The ^{13}C NMR chemical shifts for the resonances assigned to the ipso carbon atoms for **3** and **4** were found at 31.1 and 27.8 ppm, respectively. These resonances show a dramatic high-field shift compared to those for unstrained species, which is characteristic of [1]ferrocenophanes.[14] Due to its limited solubility and the long spin−lattice relaxation time (T_1) of the Si nucleus (no α-protons for polarization transfer), the ^{29}Si NMR spectrum of **3** was difficult to obtain and required a very long pulse delay and long acquisition time. The single resonance detected for **3** at −16.6 ppm is upfield of the phenylated [1]silaferrocenophane $Fe(\eta\text{-}C_5H_4)_2SiPh_2$ (δ −11.7 ppm). Interestingly, the ^{29}Si resonance of tetraferrocenylsilane **6** also lies downfield at −10.1 ppm (CD_2Cl_2). The additional shielding observed in **3** might be attributed to a weak dative Fe- - -Si interaction and is consistent with the single-crystal X-ray structure and Mössbauer data (vide supra). Both **3** and **4** have UV−vis absorptions between 480 and 490 nm typical of [1]-ferrocenophanes. In contrast, **6** has λ_{max} = 452 nm, similar to that for other unstrained ferrocene derivatives.

Spirocyclic metalloarenophanes bridged by silacyclobutane rings (**7** and **8**) were first synthesized by

(11) MacLachlan, M. J.; Lough, A. J.; Manners, I. *Macromolecules* **1996**, *29*, 8562.
(12) MacLachlan, M. J.; Kulbaba, K.; Manners, I. Manuscript in preparation.
(13) Osborne, A. G.; Whiteley, R. H. *J. Organomet. Chem.* **1975**, *101*, C27.
(14) Osborne, A. G.; Whiteley, R. H.; Meads, R. E. *J. Organomet. Chem.* **1980**, *193*, 345.
(15) Blake, A. J.; Mayers, F. R.; Osborne, A. G.; Rosseinsky, D. R. *J. Chem. Soc., Dalton Trans.* **1982**, 2379.
(16) Rosseinsky, D. R.; Osborne, A. G.; Mayers, F. R. *Opt. Mater.* **1996**, *6*, 83.
(17) Rosenberg, H. U.S. Patent 3,410,883, 1968; *Chem. Abstr.* **1969**, 13149w.

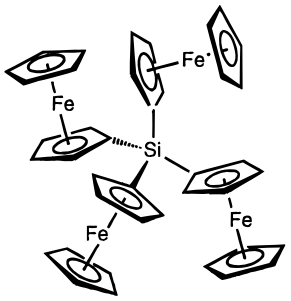

6

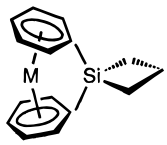

7 (M = V)
8 (M = Cr)

Elschenbroich in 1995.[18] These mononuclear species were used as control compounds in the study of metal−metal interactions in dinuclear compounds bridged by disilacyclobutane moieties. Silacyclobutanes are known to undergo thermal or transition-metal-catalyzed ROP, and their polymerization behavior has recently been reviewed.[19] We anticipated that incorporation of a ferrocenophane ring and a silacyclobutane ring into the same molecule should afford a tetrafunctional monomer suitable as a cross-linking agent for poly(ferrocenes).

The reaction of $Fe(\eta\text{-}C_5H_4Li)_2$·TMEDA with an excess of $Cl_2Si(CH_2)_3$ afforded red, hygroscopic, air-sensitive needles of **5**. Both the ^1H and ^{13}C NMR chemical shifts were consistent with the assigned structure; the ^{13}C resonance of the ipso carbon atoms was observed at 31.9 ppm. The ^{29}Si NMR spectrum showed one singlet, at 3.6 ppm; this is shifted upfield from the resonance at 18.3 ppm observed in dichlorosilacyclobutane and downfield from the resonance at −4.6 ppm for **1a**. The UV−vis spectrum of **5** shows a peak at 482 nm with a weak shoulder at shorter wavelength. In addition, the mass spectra of **3**−**6** were all consistent with their structures, giving the molecular ion as the dominant peak.

X-ray Structures of the [1]Silaferrocenophane 3 and the [1]Germaferrocenophane 4. As no previous crystallographic data for spirocyclic [1]ferrocenophanes had been reported, single-crystal X-ray diffraction studies of **3** and **4** were undertaken. Orange-red prisms of **3** suitable for X-ray diffraction were grown at −55 °C from a solution of the compound in CH_2Cl_2 and hexanes (ca. 1:1). Red crystals of **4** were obtained by slow evaporation from a solution of **4** in C_6D_6 inside a glovebox. Figures 1 and 2 show views of the molecular structures of **3** and **4**, respectively. A summary of cell contents and data collection parameters is included in Table 1, and selected bond lengths and bond angles are listed in Tables 2 and 3. A summary of important structural features for **3** and **4** is presented in Table 4.

Both **3** and **4** crystallize in the same space group (*C*2/*c*) and are isostructural. The Si and Ge atoms lie on special positions (on a 2-fold axis) in the unit cell, reflecting the C_{2v} symmetry of the molecule. To accommodate the larger atomic size of Ge (covalent radius of 122 pm for Ge vs 117 pm for Si), the unit cell of **4** is ca. 2% larger (by volume) than **3**. Similarly, the Fe- - -Fe distance in **4** (5.518(4) Å) is greater than in **3** (5.314(1)

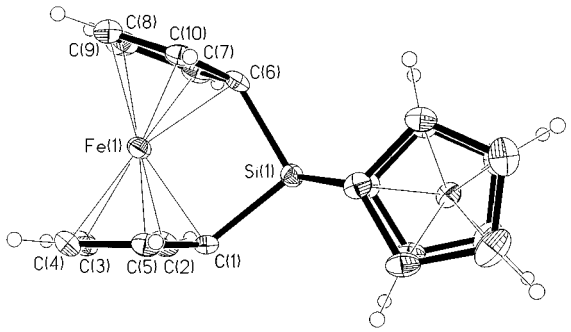

Figure 1. Molecular structure of the spirocyclic [1]-ferrocenophane **3** (thermal ellipsoids drawn at the 50% probability level).

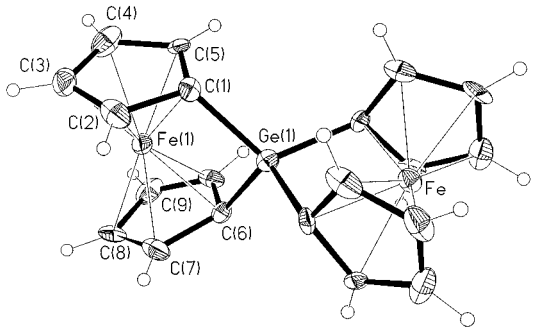

Figure 2. Molecular structure of the spirocyclic [1]-ferrocenophane **4** (thermal ellipsoids drawn at the 50% probability level).

Å). The Cp rings of both **3** and **4** are eclipsed (torsion angles of 1.1 and 0.8°, respectively) and are essentially planar; mean deviations of 0.002 and 0.005 Å from the plane containing C(1)−C(5) and 0.003 and 0.003 Å for the C(6)−C(10) plane are present in **3** and **4**, respectively. The tilting of the planes of the cyclopentadienyl ligands with respect to one another in **3** (α = 19.4(2)°) is less than in **1a** (α = 20.8(5)°),[20] indicating that introduction of a second ferrocenophane ring at silicon slightly reduces the ring tilt observed. On the other hand, the ring tilt of **4** (α = 19.1(5)°) is similar to the ring tilts of **3** and **1b** (α = 19.0(9)°),[21] although the large estimated standard deviations of the angles for **1b** and **4** make meaningful comparisons difficult. The Si−C_{ipso} bond lengths in **3** (1.871(3) and 1.874(3) Å) are similar to the bond lengths in **1a** (1.858(9) Å) and tetraferrocenylsilane **6** (1.851(7)−1.870(6) Å) (see below). Likewise, the Ge−C_{ipso} bond lengths in **4** (1.952(9) Å) are only slightly shorter than the same bond lengths in **1b** (1.978(6) Å). The values of the angle β between the planes of the Cp ligands and the C_{ipso}−bridging atom bonds for **3** and **1a** indicate that **3** possesses a larger distortion from planarity at the ipso carbon atom than does **1a** (β = 39.5(1)° for **3**, β = 37.0(6)° for **1a**). For ferrocenophane **4**, the β angle is 37.5(4)°, consistent with the value for **1b** (β = 37.0(6)°). While the C−C−C angles in the Cp ring of ferrocene are 108°, there is a small distortion from a perfect pentagon in the Cp rings of **3** and **4**. The C_{ipso}−E−C_{ipso} bond angles in **3** (98.5(1)°) and **4** (94.7(4)°) are significantly smaller than the ideal

(18) Elschenbroich, C.; Bretschneider-Hurley, A.; Hurley, J.; Behrendt, A.; Massa, W.; Wocadlo, S.; Reijerse, E. *Inorg. Chem.* **1995**, *34*, 743.
(19) Ushakov, N. V.; Finkel'shtein, E. S.; Babich, E. D. *Polym. Sci., Ser. A* **1995**, *37*, 320.
(20) Finckh, W.; Tang, B.-Z.; Foucher, D. A.; Zamble, D. B.; Ziembinski, R.; Lough, A.; Manners, I. *Organometallics* **1993**, *12*, 823.
(21) Foucher, D. A.; Edwards, M.; Burrow, R. A.; Lough, A. J.; Manners, I. *Organometallics* **1994**, *13*, 4959.

Table 1. Summary of Crystal Data and Data Collection Parameters for 3−6

	3	4	5	6
empirical formula	$C_{20}H_{16}Fe_2Si$	$C_{20}H_{16}Fe_2Ge$	$C_{13}H_{14}FeSi$	$C_{40}H_{36}Fe_4Si$
M_r	396.12	440.62	254.18	768.18
temp (K)	168(2)	168(2)	168(2)	168(2)
wavelength (Å)	0.710 73	0.710 73	0.710 73	0.710 73
cryst syst	monoclinic	monoclinic	monoclinic	orthorhomic
space group	*C*2/*c*	*C*2/*c*	$P2_1/n$	$Pca2_1$
a, Å	20.771(2)	21.130(9)	10.603(2)	15.326(2)
b, Å	10.304(1)	10.293(4)	6.085(1)	14.087(1)
c, Å	7.424(1)	7.437(4)	17.210(2)	14.590(2)
β, deg	100.99(1)	100.61(1)	98.60(1)	90
V, Å^3	1559.8(3)	1589.8(13)	1097.9(3)	3149.9(6)
Z	4	4	4	4
D_{calc}, g cm^{-3}	1.687	1.841	1.538	1.620
μ(Mo Kα), cm^{-1}	19.31	36.73	14.42	18.73
F(000)	808	880	528	1576
cryst size (mm)	0.3 × 0.3 × 0.1	0.2 × 0.2 × 0.05	<0.5 × 0.5 × 0.5	0.31 × 0.15 × 0.15
θ range collected, deg	3.41−27.00	3.41−26.00	3.56−30.00	2.66−27.00
total no. of rflns	1748	1603	3365	3573
no. of unique rflns	1703	1562	3209	3573
weighting scheme *a*[a]	0.0331	0.0505	0.0399	0.0236
R_{int}	0.0372	0.0710	0.0236	0.0000
abs cor	semiempirical	semiempirical	semiempirical	semiempirical
wR2 (all data)	0.0747	0.1283	0.0713	0.0764
R1 ($I > 2\sigma(I)$)	0.0317	0.0511	0.0266	0.0377
GOF	0.838	0.870	1.012	0.850
$(\Delta/\sigma)_{max}$ in last cycle	0.000	0.088	0.001	0.002
no. of params	130	106	178	408
residual electron density (e Å^{-3})	+0.395/−0.290	+0.737/−0.673	+0.444/−0.412	+0.313/−0.357
extinction coeff	0.0020(2)	0.0000(2)	none	0.00036(6)
abs struct param				−0.13(6)

[a] Weight = $1/[\sigma^2(F_o)^2 + (aP)^2]$, where $P = (\mathrm{Max}(F_o^2,0) + 2F_c^2)/3$.

Table 2. Selected Bond Lengths (Å) and Angles (deg) for 3

Distances			
Fe(1)−Si(1)	2.6572(5)	Si(1)−C(6)	1.871(3)
Fe(1)−C(1)	2.017(3)	C(1)−C(2)	1.441(4)
Fe(1)−C(2)	2.032(3)	C(1)−C(5)	1.448(4)
Fe(1)−C(3)	2.084(3)	C(2)−C(3)	1.429(5)
Fe(1)−C(4)	2.075(3)	C(3)−C(4)	1.423(5)
Fe(1)−C(5)	2.027(3)	C(4)−C(5)	1.422(5)
Fe(1)−C(6)	2.019(3)	C(6)−C(7)	1.450(4)
Fe(1)−C(7)	2.028(3)	C(6)−C(10)	1.451(4)
Fe(1)−C(8)	2.068(3)	C(7)−C(8)	1.421(5)
Fe(1)−C(9)	2.077(3)	C(8)−C(9)	1.420(5)
Fe(1)−C(10)	2.031(3)	C(9)−C(10)	1.413(5)
Si(1)−C(1)	1.874(3)		
Angles			
Si(1)−C(1)−C(2)	119.7(2)	C(2)−C(1)−C(5)	105.5(3)
Si(1)−C(1)−C(5)	116.3(2)	C(3)−C(4)−C(5)	108.1(3)
Si(1)−C(6)−C(7)	118.4(2)	C(6)−C(7)−C(8)	108.9(3)
Si(1)−C(6)−C(10)	117.9(2)	C(6)−C(10)−C(9)	109.7(3)
C(1)−Si(1)−C(6)	98.48(12)	C(7)−C(8)−C(9)	108.5(3)
C(1)−C(2)−C(3)	109.4(3)	C(7)−C(6)−C(10)	105.1(3)
C(1)−C(5)−C(4)	109.3(3)	C(8)−C(9)−C(10)	107.8(3)
C(2)−C(3)−C(4)	107.7(3)		

Table 3. Selected Bond Lengths (Å) and Angles (deg) for 4

Distances			
Fe(1)−Ge(1)	2.759(2)	Ge(1)−C(6)	1.955(9)
Fe(1)−C(1)	2.021(9)	C(1)−C(2)	1.461(12)
Fe(1)−C(2)	2.021(9)	C(1)−C(5)	1.422(11)
Fe(1)−C(3)	2.089(10)	C(2)−C(3)	1.436(14)
Fe(1)−C(4)	2.082(10)	C(3)−C(4)	1.432(14)
Fe(1)−C(5)	2.026(8)	C(4)−C(5)	1.420(12)
Fe(1)−C(6)	2.041(9)	C(6)−C(7)	1.472(12)
Fe(1)−C(7)	2.057(8)	C(6)−C(10)	1.433(13)
Fe(1)−C(8)	2.085(8)	C(7)−C(8)	1.441(13)
Fe(1)−C(9)	2.081(9)	C(8)−C(9)	1.447(13)
Fe(1)−C(10)	2.030(9)	C(9)−C(10)	1.391(14)
Ge(1)−C(1)	1.948(9)		
Angles			
Ge(1)−C(1)−C(2)	118.9(7)	C(2)−C(1)−C(5)	105.8(8)
Ge(1)−C(1)−C(5)	117.9(6)	C(3)−C(4)−C(5)	108.9(9)
Ge(1)−C(6)−C(7)	117.5(7)	C(6)−C(7)−C(8)	107.7(8)
Ge(1)−C(6)−C(10)	118.8(6)	C(6)−C(10)−C(9)	110.9(8)
C(1)−Ge(1)−C(6)	94.7(4)	C(7)−C(8)−C(9)	107.6(8)
C(1)−C(2)−C(3)	109.3(9)	C(7)−C(6)−C(10)	105.7(8)
C(1)−C(5)−C(4)	109.6(8)	C(8)−C(9)−C(10)	108.1(9)
C(2)−C(3)−C(4)	106.4(9)		

tetrahedral value (109.5°), consistent with the analogous angles in other [1]silaferrocenophanes and [1]germaferrocenophanes. However, these angles are larger than in **1a** (95.7(4)°) and **1b** (91.7(3)°), suggesting that the Si and Ge tetrahedral environments are less distorted in **3** and **4**. It is probably the combination of near-tetrahedral geometry at the bridging atom and the steric hindrance imparted by four Cp rings that is responsible for the unusual air and moisture stability in these [1]-ferrocenophanes.

X-ray Structure of Tetraferrocenylsilane 6. A search of the Cambridge Structural Database revealed that no other compounds containing a silicon atom attached to four Cp ligands have been characterized by X-ray crystallography. A structural investigation of tetraferrocenylsilane was undertaken to permit a comparison with the spirocyclic [1]silaferrocenophane **3**. Crystals of **6** were obtained by slow evaporation of a solution of **6** in C_6D_6 under a nitrogen atmosphere. Figure 3 gives a view of the molecular structure of **6**. The cell contents and data collection parameters are summarized in Table 1, and selected bond lengths and bond angles are listed in Table 5.

Despite the apparent symmetry of **6**, it crystallizes in the chiral, orthorhombic space group $Pca2_1$, where the molecule possesses no symmetry elements. The chirality of the structure was determined unambiguously by X-ray diffraction, as indicated by the small

Table 4. Selected Structural Data for [1]Ferrocenophanes

	1a	3	5	1b	4
Fe−E dist, Å	2.690(3)	2.6572(5)	2.7113(5)	2.804(2)	2.759(2)
$\Sigma(r_{Fe} + r_x)$,[a] Å	2.41	2.41	2.41	2.47	2.47
Fe displacement,[b] Å	0.216(1)	0.210(3)	0.222(2)	0.221(9)	0.214(9)
ring tilt, α, deg	20.8(5)	19.4(2)	20.61(8)	19.0(9)	19.1(5)
β,[c] deg	37.0(6)	39.5(1)	37.4(1)	36.8(5)	37.5(5)
C1−E−C6, θ, deg	95.7(4)	98.5(1)	95.83(6)	91.7(3)	94.7(4)
Cp−Fe−Cp, δ, deg	164.74(8)	165.3(2)	164.4(1)	165.3(5)	165.1(4)
ref	20	this work	this work	21	this work

[a] Sum of the covalent radii of Fe and the bridging atom E. [b] Displacement of the iron atom from the line joining the two centroids of the cyclopentadienyl rings. [c] Average of the angle(s) between the planes of the cyclopentadienyl ligands and the C(Cp)−E bonds (where E = bridging atom).

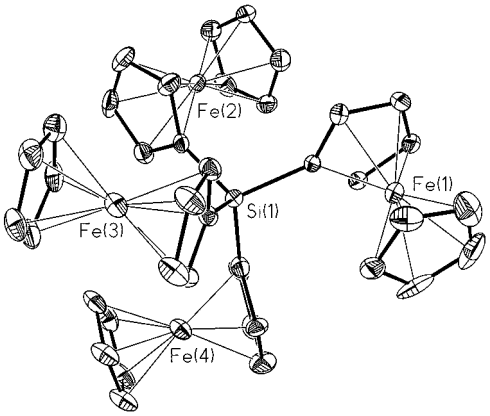

Figure 3. Molecular structure of **6** (thermal ellipsoids drawn at the 25% probability level).

absolute structure factor. This rigid, chiral conformation is probably induced by the steric demands of the ferrocenyl substituents at Si. One can view the structure as a pinwheel of three ferrocenes with the fourth ferrocene attached above the plane. The Fe- - -Fe separation varies from 5.27 to 6.14 Å between the ferrocenes. Each of the Cp ligands is essentially planar, with very slight ring tilts of 0.7(5), 1.3(5), 2.4(5), and 3.6(6)° observed for the ferrocenyl substituents. Notably, values of the angle β between the planes of the Cp ligands and the C_{ipso}−bridging atom bonds in **6** are 3.0(6), 4.3(6), 4.9(6), and 6.6(6)°. This small distortion from ideal sp^2 hybridization of the ipso carbon atoms is likely also the result of steric crowding around Si.

^{57}Fe Mössbauer Spectra of 3, 4, and 6. Mössbauer spectra of ferrocene derivatives can provide valuable insight into the Fe environments. Studies of [1]ferrocenophanes have indicated a reduction in quadrupolar splitting relative to ferrocene (2.31 mm s^{-1}), while the isomer shift is similar (0.43 mm s^{-1}) (data relative to Fe powder). Silver has attributed the quadrupolar splitting shift to a weak iron-to-heteroatom interaction.[22] Osborne et al. reported the Mössbauer spectroscopic data for **3** at 77 K; these workers measured the isomer shift δ of 0.51 mm s^{-1} and the quadrupolar splitting value ΔE_q of 2.01 mm s^{-1}.[14] At room temperature, we found the isomer shift value δ (relative to Fe powder) for **3** was 0.442(5) mm s^{-1}, while the quadrupolar splitting value ΔE_q was 2.013(5) mm s^{-1}. The corresponding values for **4** were δ = 0.454(5) mm s^{-1} and ΔE_q = 2.090(5) mm s^{-1}. This postulate for a weak dative interaction between the Fe and the bridging atom[22] is consistent with the ^{29}Si NMR data, where the ^{29}Si resonance of **3** (−16.6 ppm) is upfield from that of **6** (−10.1 ppm). However, it was predicted that the quadrupolar splitting values for **3** and **4** might be significantly higher than those for other [1]sila- and [1]germaferrocenophanes, respectively, because the atom bridging the two ferrocenophanes would be unable to accommodate the same degree of electron density from the two Fe centers as in other [1]ferrocenophanes. The observation that **3** and **4** have quadrupolar splitting values similar to those of other [1]ferrocenophanes suggests that other factors, such as changes in bonding in the ferrocenophane due to ring tilting and C_{ipso} distortion, may be required to explain the quadrupolar splittings. As expected, the Mössbauer spectroscopic data for **6** are very similar to those for ferrocene, where the measured isomer shift value δ (relative to Fe powder) was 0.429(5) mm s^{-1} and the quadrupolar splitting value ΔE_q was 2.262(5) mm s^{-1}.

X-ray Structure of 5. Single crystals of **5** suitable for X-ray diffraction were obtained by solvent evaporation from the filtered reaction mixture. Figure 4 shows the molecular structure of **5**. A summary of cell constants and data collection parameters is included in Table 1, and important bond lengths and angles are listed in Table 6. A summary of important structural features is presented in Table 4.

As in **3** and **4**, the two cyclopentadienyl rings of **5** are virtually eclipsed, and each is essentially planar with an observed mean deviation from the plane of 0.004 Å calculated by a weighted least-squares plane through the cyclopentadienyl ligand containing C(1)−C(5), with the same value for the cyclopentadienyl ligand containing C(6)−C(10). The Cp rings are tilted with respect to one another in **5** (α = 20.61(8)°) to a similar degree as in **1a** (α = 20.8(5)°). The Si−C_{ipso} bond lengths in **5** (1.883(2) and 1.884(2) Å) are in accord with those in other [1]silaferrocenophanes such as **1a**. The value of the angle β between the planes of the Cp ligands and the C_{ipso}−Si bond for **5** (β = 37.4(1)°) indicates a large distortion from the linear sp^2 hybridization at the C_{ipso} atom. The C_{ipso}−Si−C_{ipso} bond angle in **5** (95.83(6)°) is also significantly less than the tetrahedral value (109.5°) and agrees with the value for **1a** (95.7(4)°). In **1a**, a scissoring effect is observed, giving rise to a wider C_{Me}−Si−C_{Me} angle (114.8(6)°) than expected for a tetrahedral geometry. In **5**, however, the C(11)−Si−C(13) angle (81.10(8)°) is constrained by the silacyclobutane ring. This leaves a large part of the Si atom exposed and may explain why **5** is very moisture sensitive. The Fe- - -Si distance in **5** (2.7113(5) Å) is only slightly longer than in **1a** (2.690(3) Å) but is significantly longer than in **3**

(22) Roberts, R. M. G.; Silver, J.; Ranson, R. J.; Morrison, I. E. G. *J. Organomet. Chem.* **1981**, *219*, 233.

Table 5. Selected Bond Lengths (Å) and Angles (deg) for 6

Distances			
Fe(1)−C(1)	2.064(6)	Si(1)−C(21)	1.869(7)
Fe(1)−C(2)	2.047(8)	Si(1)−C(31)	1.853(7)
Fe(1)−C(3)	2.051(6)	C(1)−C(2)	1.441(8)
Fe(1)−C(4)	2.056(7)	C(1)−C(5)	1.424(9)
Fe(1)−C(5)	2.038(6)	C(2)−C(3)	1.438(10)
Fe(1)−C(6)	2.058(7)	C(3)−C(4)	1.423(9)
Fe(1)−C(7)	2.027(8)	C(4)−C(5)	1.422(9)
Fe(1)−C(8)	2.022(9)	C(6)−C(7)	1.415(11)
Fe(1)−C(9)	2.028(9)	C(6)−C(10)	1.391(10)
Fe(1)−C(10)	2.044(8)	C(7)−C(8)	1.379(14)
Fe(2)−C(11)	2.061(6)	C(8)−C(9)	1.39(2)
Fe(2)−C(12)	2.022(7)	C(9)−C(10)	1.361(13)
Fe(2)−C(13)	2.053(6)	C(11)−C(12)	1.398(9)
Fe(2)−C(14)	2.061(8)	C(11)−C(15)	1.434(9)
Fe(2)−C(15)	2.057(7)	C(12)−C(13)	1.445(10)
Fe(2)−C(16)	2.017(7)	C(13)−C(14)	1.425(12)
Fe(2)−C(17)	2.016(8)	C(14)−C(15)	1.403(9)
Fe(2)−C(18)	2.041(8)	C(16)−C(17)	1.394(10)
Fe(2)−C(19)	2.033(7)	C(16)−C(20)	1.397(10)
Fe(2)−C(20)	2.045(7)	C(17)−C(18)	1.387(9)
Fe(3)−C(21)	2.061(7)	C(18)−C(19)	1.406(11)
Fe(3)−C(22)	2.041(7)	C(19)−C(20)	1.412(10)
Fe(3)−C(23)	2.046(9)	C(21)−C(22)	1.429(8)
Fe(3)−C(24)	2.028(8)	C(21)−C(25)	1.438(9)
Fe(3)−C(25)	2.019(8)	C(22)−C(23)	1.414(9)
Fe(3)−C(26)	2.047(8)	C(23)−C(24)	1.443(10)
Fe(3)−C(27)	2.046(8)	C(24)−C(25)	1.405(9)
Fe(3)−C(28)	2.044(7)	C(26)−C(27)	1.404(10)
Fe(3)−C(29)	2.045(7)	C(26)−C(30)	1.388(11)
Fe(3)−C(30)	2.051(8)	C(27)−C(28)	1.394(10)
Fe(4)−C(31)	2.060(8)	C(28)−C(29)	1.425(11)
Fe(4)−C(32)	2.048(7)	C(29)−C(30)	1.399(10)
Fe(4)−C(33)	2.048(7)	C(31)−C(32)	1.451(9)
Fe(4)−C(34)	2.024(8)	C(31)−C(35)	1.454(9)
Fe(4)−C(35)	2.046(8)	C(32)−C(33)	1.422(10)
Fe(4)−C(36)	2.052(8)	C(33)−C(34)	1.414(11)
Fe(4)−C(37)	2.036(9)	C(34)−C(35)	1.432(9)
Fe(4)−C(38)	2.057(8)	C(36)−C(37)	1.447(10)
Fe(4)−C(39)	2.067(8)	C(36)−C(40)	1.423(10)
Fe(4)−C(40)	2.066(8)	C(37)−C(38)	1.405(12)
Si(1)−C(1)	1.866(6)	C(38)−C(39)	1.400(11)
Si(1)−C(11)	1.870(6)	C(39)−C(40)	1.432(10)

Angles			
C(1)−Si(1)−C(11)	108.5(3)	C(12)−C(13)−C(14)	106.6(7)
C(1)−Si(1)−C(21)	109.2(3)	C(13)−C(14)−C(15)	107.9(7)
C(1)−Si(1)−C(31)	106.1(3)	C(16)−C(17)−C(18)	108.6(7)
C(11)−Si(1)−C(21)	109.4(3)	C(16)−C(20)−C(19)	108.0(7)
C(11)−Si(1)−C(31)	111.7(3)	C(17)−C(16)−C(20)	108.0(7)
C(21)−Si(1)−C(31)	111.9(3)	C(17)−C(18)−C(19)	108.3(7)
Si(1)−C(1)−C(2)	124.3(5)	C(18)−C(19)−C(20)	107.1(7)
Si(1)−C(1)−C(5)	129.5(5)	C(21)−C(22)−C(23)	110.7(6)
Si(1)−C(11)−C(12)	124.4(6)	C(21)−C(25)−C(24)	110.0(7)
Si(1)−C(11)−C(15)	129.0(5)	C(22)−C(21)−C(25)	105.0(6)
Si(1)−C(21)−C(22)	130.2(5)	C(22)−C(23)−C(24)	106.4(7)
Si(1)−C(21)−C(25)	124.6(5)	C(23)−C(24)−C(25)	107.9(7)
Si(1)−C(31)−C(32)	128.5(6)	C(26)−C(27)−C(28)	109.3(8)
Si(1)−C(31)−C(35)	125.0(5)	C(26)−C(30)−C(29)	108.4(8)
C(1)−C(2)−C(3)	108.6(6)	C(27)−C(26)−C(30)	107.7(7)
C(1)−C(5)−C(4)	109.8(6)	C(27)−C(28)−C(29)	106.4(7)
C(2)−C(1)−C(5)	106.2(6)	C(28)−C(29)−C(30)	108.2(7)
C(2)−C(3)−C(4)	107.6(6)	C(31)−C(32)−C(33)	108.2(7)
C(3)−C(4)−C(5)	107.8(6)	C(31)−C(35)−C(34)	108.9(7)
C(6)−C(7)−C(8)	108.9(10)	C(32)−C(31)−C(35)	105.9(6)
C(6)−C(10)−C(9)	109.2(9)	C(32)−C(33)−C(34)	109.5(7)
C(7)−C(6)−C(10)	105.7(9)	C(33)−C(34)−C(35)	107.4(7)
C(7)−C(8)−C(9)	107.1(10)	C(36)−C(37)−C(38)	106.9(7)
C(8)−C(9)−C(10)	109.1(10)	C(36)−C(40)−C(39)	108.4(7)
C(11)−C(12)−C(13)	109.5(8)	C(37)−C(36)−C(40)	107.3(7)
C(11)−C(15)−C(14)	109.6(8)	C(37)−C(38)−C(39)	110.4(8)
C(12)−C(11)−C(15)	106.5(6)	C(38)−C(39)−C(40)	107.0(8)

(2.6572(5) Å). There is possibly a weak interaction between the Fe and Si atoms in **5**, just as has been proposed for other [1]silaferrocenophanes. The carbosilane ring in **5** is also clearly strained with skeletal

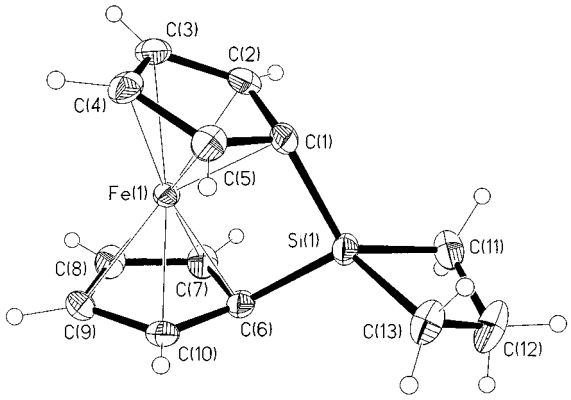

Figure 4. Molecular structure of **5** (thermal ellipsoids drawn at the 50% probability level).

Table 6. Selected Bond Lengths (Å) and Angles (deg) for 5

Distances			
Fe(1)−Si(1)	2.7113(5)	Si(1)−C(13)	1.869(2)
Fe(1)−C(1)	2.0135(14)	C(1)−C(2)	1.450(2)
Fe(1)−C(2)	2.026(2)	C(1)−C(5)	1.450(2)
Fe(1)−C(3)	2.079(2)	C(2)−C(3)	1.424(2)
Fe(1)−C(4)	2.0772(14)	C(3)−C(4)	1.418(2)
Fe(1)−C(5)	2.0303(14)	C(4)−C(5)	1.433(2)
Fe(1)−C(6)	2.0131(14)	C(6)−C(7)	1.445(2)
Fe(1)−C(7)	2.027(2)	C(6)−C(10)	1.449(2)
Fe(1)−C(8)	2.074(2)	C(7)−C(8)	1.426(2)
Fe(1)−C(9)	2.0775(14)	C(8)−C(9)	1.417(2)
Fe(1)−C(10)	2.0248(14)	C(9)−C(10)	1.428(2)
Si(1)−C(1)	1.884(2)	C(11)−C(12)	1.556(3)
Si(1)−C(6)	1.883(2)	C(12)−C(13)	1.560(3)
Si(1)−C(11)	1.870(2)	Si(1)−C(12)	2.358(2)

Angles			
Si(1)−C(1)−C(2)	120.48(12)	C(1)−C(2)−C(3)	109.52(14)
Si(1)−C(1)−C(5)	117.54(11)	C(1)−C(5)−C(4)	109.25(14)
Si(1)−C(6)−C(7)	118.99(11)	C(2)−C(3)−C(4)	108.18(13)
Si(1)−C(6)−C(10)	119.06(11)	C(2)−C(1)−C(5)	105.13(12)
Si(1)−C(11)−C(12)	86.45(11)	C(3)−C(4)−C(5)	107.92(14)
Si(1)−C(13)−C(12)	86.39(11)	C(6)−C(7)−C(8)	109.6(2)
C(1)−Si(1)−C(6)	95.83(6)	C(6)−C(10)−C(9)	109.43(14)
C(1)−Si(1)−C(11)	124.39(8)	C(7)−C(8)−C(9)	108.04(14)
C(1)−Si(1)−C(13)	121.11(8)	C(7)−C(6)−C(10)	105.09(13)
C(6)−Si(1)−C(11)	118.15(7)	C(8)−C(9)−C(10)	107.89(14)
C(6)−Si(1)−C(13)	118.68(8)	C(11)−C(12)−C(13)	102.59(13)
C(11)−Si(1)−C(13)	81.10(8)		

C−Si−C and C−C−C bond angles significantly less than 109.5°. Interestingly, the silacyclobutane ring in **5** is puckered[23] by only 20.6(2)° from planarity, significantly less than in bis(η^5-benzene)vanadium **7** (23°)[18] and 4-sila-3,3-spiroheptane, $(CH_2)_3Si(CH_2)_3$ (30(2)° by electron diffraction[24]).

Cyclic Voltammetry of 3−6. Cyclic voltammetry (CV) of **5** showed a single, reversible oxidation with $E_{1/2}$ = 0.11 V vs ferrocene in CH_2Cl_2. This is typical of [1]silaferrocenophanes; for example, **1a** exhibits a single reversible oxidation with $E_{1/2}$ = 0.00 V with respect to the ferrocene/ferrocenium couple.[25] CV of **3** showed two oxidations. The first, with $E_{1/2}$ = 0.14 V, corresponds to the formation of the mixed-valent Fe^{II}/Fe^{III} compound; this wave was reversible at all of the scan rates studied. Surprisingly, the second oxidation, corresponding to the

(23) We define the ring pucker as the angle between the plane defined by Si, C(11), and C(13) and the plane defined by C(11), C(12), and C(13). Thus, it quantifies the fold in the silacyclobutane ring.

(24) Mastryukov, V. S.; Dorefeeva, O. V.; Vilkov, L. V.; Cyvin, S. J.; Cyvin, B. N. *J. Struct. Chem. (Engl. Transl.)* **1975**, *16*, 438.

(25) Pudelski, J. K.; Foucher, D. A.; Honeyman, C. H.; Lough, A. J.; Manners, I.; Barlow, S.; O'Hare, D. *Organometallics* **1995**, *14*, 2470.

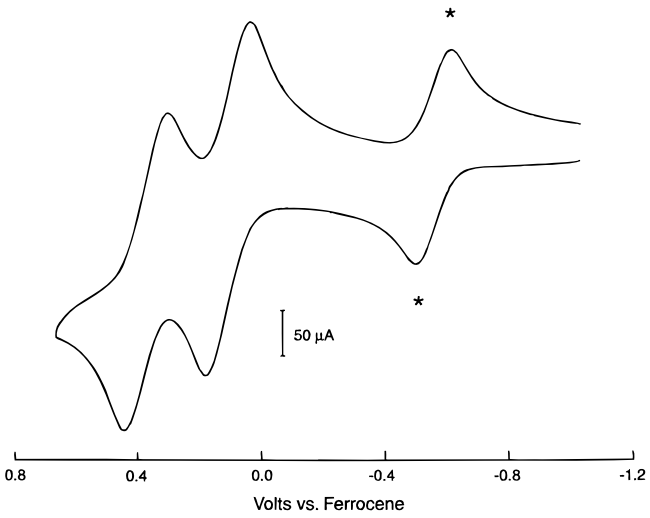

Figure 5. Cyclic voltammogram of 5 mM **4** in dichloromethane (scan rate 1.0 V s^{-1}). The peaks marked by asterisks are from the internal reference, decamethylferrocene.

formation of an Fe^{III}/Fe^{III} species, was irreversible. A large separation between the two oxidations, ΔE_{ox} = 0.37 V (scan rate 0.25 V s^{-1}), indicates a significant Fe- - -Fe interaction between the two ferrocenophane units.

CV of **4** also showed two oxidations (Figure 5). In this case, the first oxidation, at $E_{1/2}$ = 0.11 V, was reversible at all scan rates. The second oxidation at $E_{1/2}$ = 0.36 V was reversible for all scan rates faster than ca. 0.25 V s^{-1}. As expected, the $E_{1/2}$ separation, $\Delta E_{1/2}$, was less for **4** ($\Delta E_{1/2}$ = 0.25 V) than for **3** (ΔE_{ox} = 0.37 V), implying a larger Fe- - -Fe interaction for the Si bridge compared to that for Ge. Clearly, the large $\Delta E_{1/2}$ values for **3** and **4** indicate a significant Fe- - -Fe interaction in these molecules (cf. $\Delta E_{1/2}$ = 0.34 V in biferrocene[26] (CH_2Cl_2)).

Cyclic voltammetry of **6** in CH_2Cl_2 and THF provided poor resolution of the four oxidation waves. In benzonitrile, however, the four reversible oxidations were readily resolved. Figure 6 shows the cyclic voltammogram and differential pulse voltammogram of **6**. The redox potentials (versus ferrocene) for each oxidation are listed in Table 7.

Recently, a number of papers have appeared reporting the preparation and electrochemical characterization of multiply ferrocenyl-substituted complexes.[27] These studies are relevant in general to the question of how biological systems deliver several electron equivalents to redox sites.[27,28] It has been demonstrated, for example, that the four Fe centers in cytochrome c_3 undergo electron transfer at very similar potentials, the spread of the four Fe^{II}/Fe^{III} $E_{1/2}$ values being only 0.11 V.[29]

In the present work on compound **6**, the spread of the four potentials is 0.42 V, implying appreciable interactions between the ferrocenyl moieties as they are

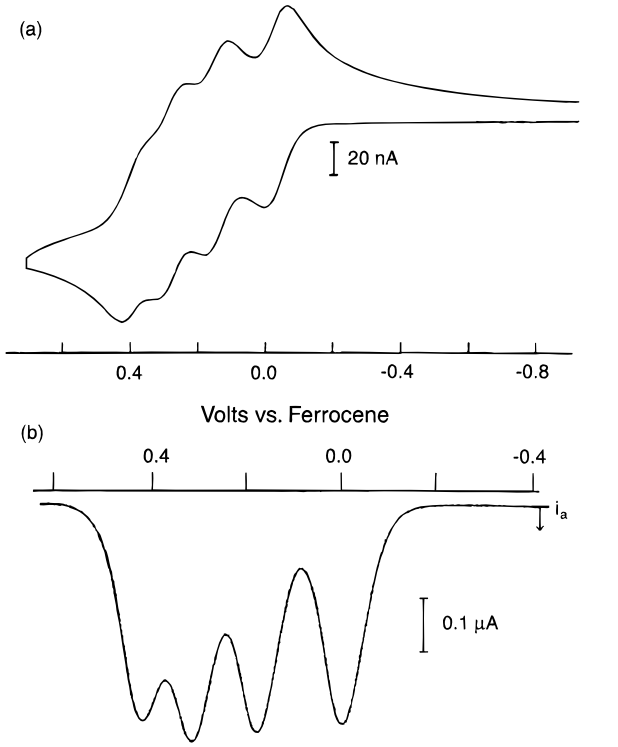

Figure 6. (a) Cyclic voltammogram of 0.31 mM **6** in benzonitrile at a Pt-disk electrode (scan rate 0.05 V s^{-1}). (b) Differential pulse voltammogram of 0.31 mM **6** in benzonitrile at a Pt-disk electrode (scan rate 2 mV s^{-1}, drop time 1 s).

Table 7. Redox Potentials of 6 from Cyclic Voltammetry

oxidn wave	$E_{1/2}$ (V vs ferrocene)[a]	oxidn wave	$E_{1/2}$ (V vs ferrocene)[a]
6/[**6**]$^+$	−0.03	[**6**]$^+$/[**6**]$^{2+}$	+0.15
[**6**]$^{2+}$/[**6**]$^{3+}$	+0.29	[**6**]$^{3+}$/[**6**]$^{4+}$	+0.39

[a] In benzonitrile. See Experimental Section for details.

successively oxidized. This fact stands in contrast to the case for $MeSi[(aryl)Cr(CO)_3]_3$, in which the oxidations of the three $Cr(CO)_3$ groups occur at virtually the same potential, implying electronic isolation of the redox centers.[30] The results for **6** are more in line with those of a multiferrocenyl analogue having boron as the bridging atom, namely fc_4B, which was formulated as the zwitterion (ferrocenium)tris(ferrocenyl)borate.[31] This complex showed four reversible one-electron oxidations with $E_{1/2}$ values (versus Ag/AgCl) of −0.18, −0.09, 0.29, and 0.41 V. The overall spread of 0.59 V is even larger than that measured for complex **6**. It may be concluded that single bridging atoms of group 13 or group 14 both allow significant interactions between ferrocenyl substituents in their multiply ferrocenyl-substituted complexes.

Vibrational Spectroscopy. The vibrational spectroscopy of [1]ferrocenophanes is unexplored. A systematic vibrational analysis of [1]ferrocenophanes may reveal trends in vibrational frequencies as a function of ring tilt, distortion from sp^2 hybridization at the C_{ipso}

(26) Brown, G. M.; Meyer, T. J.; Cowan, D. O.; Levanda, C.; Kaufman, F.; Roling, P. V.; Raush, M. D. *Inorg. Chem.* **1975**, *14*, 506.
(27) For leading references, see: Tendero, M. J. L.; Benito, A.; Cano, J.; Lloris, J. M.; Martinez-Manez, R.; Soto, J.; Edwards, A. J.; Raithby, P. R.; Rennie, M. A. *J. Chem. Soc., Chem. Commun.* **1995**, 1643.
(28) Steiger, B.; Shi, C.; Anson, F. C. *Inorg. Chem.* **1993**, *32*, 2107.
(29) Sokol, W. F.; Evans, D. H.; Niki, K.; Yagi, T. *J. Electroanal. Chem. Interfacial Electrochem.* **1980**, *108*, 107.
(30) Reike, R. D.; Tucker, I.; Milligan, S. N.; Wright, D. R.; Willeford, B. R.; Radnovich, L. J.; Eyring, M. W. *Organometallics* **1982**, *1*, 938.
(31) Cowan, D. O.; Shu, P.; Hedberg, F. L.; Rossi, M.; Kistenmacher, T. J. *J. Am. Chem. Soc.* **1979**, *101*, 1304.

Table 8. Infrared Bands of 3 and 4

3	4	assignt[a]
3095 w	3095 w	ν_{C-H} (sym)
3081 w	3081 w	ν_{C-H}
2851 w		
	1292 m	
1178 m	1182 s	$\delta_{C-H_{ip}}$
	1154 w	
1119 w		
1123 m	1114 s	sym ring breath
1032 s	1021 s	$\delta_{C-H_{oop}}$
1019 m		$\delta_{C-H_{ip}}$
1013 m	1006 w	
890 m	888 w	ring distortion
880 s, 882 s	876 s	
856 w	852 w	
852 m	848 m	$\delta_{C-H_{oop}}$
827 w	832 w	
815 w	815 w	
805 s, 802 s	803 s	$\delta_{C-H_{oop}}$
	690 w	
696 m	661 m	
596 w	594 w	$\delta_{C-C_{oop}}$
567s		
536 m	531 m	
513 m		
510 m	510 s	
	505 m	

[a] Legend: ν = stretch; δ = bend; ip = in plane; oop = out of plane

Table 9. Raman Bands of 3, 4, 6, and Ferrocene

3	4	6	ferrocene[a]	assignt[b]
3099 s	3099 s	3112 s	3100 s	ν_{C-H}(sym)
3086 m	3086 m	3092 m	3085 w	ν_{C-H}
3077 w	3077 w		3070 w	ν_{C-H}
1400 m	1401 m	1418 m	1412 m	ν_{C-C}(sym)
1378 m	1376 m	1383 w		ν_{C-C}
		1369 w		
1349 w	1347 w	1357 w	1356 w	ν_{C-C}
1180 w	1187 w	1194 w	1175 w	$\delta_{C-H_{ip}}$
		1159 m		
1119 s	1116 s	1111 s	1105 s	sym ring breath
1060 s	1060 s	1065 m	1059 m	$\delta_{C-H_{oop}}$
1046 vw	1046 vw	1040w		
1023 w	1021 w			$\delta_{C-H_{ip}}$
1017 w	1009 w	1005 w	999 w	$\delta_{C-H_{ip}}$
901 vw	898 vw	888 w	892 w	ring distortion
878 m	873 m			
854 vw	851 vw			
838 vw	836 vw		835 w	$\delta_{C-H_{oop}}$
817 vw	816 vw			$\delta_{C-H_{oop}}$
807 vw	805 vw			
723 vw				
714 m				
	689 m			
594 vw	593 vw	615 w	600 w	$\delta_{C-C_{oop}}$
556 w				
539 w	535 w			Cp−Fe−Cp deform
450 vw				
	435 m			
422 s	419 s			
	403 m	410 m		
397 vs	390 vs	398 m	390 s	ring tilt (sym)
	335 w	333 m		
325 s	292 s	316 s	301 s	ν_{Fe-Cp}(sym)
256 m		265 m		
248 s	246 s	248 w		
241 w				
234 m	228 w	231 w		
	184 vw			
143 vw	142 vw			

[a] Reference 32. [b] Legend: ν = stretch; δ = bend; ip = in plane; oop = out of plane

atom, or other geometric properties. Furthermore, these techniques offer the possibility of examining structural dynamics in solution and the gas phase. To corroborate the structures of the spirocyclic molecules **3** and **4**, both IR and Raman spectra were obtained. Table 8 lists the IR absorption frequencies for compounds **3** and **4**, along with tentative peak assignments. Table 9 presents the Raman peaks for compounds **3**, **4**, and **6** with their tentative assignments.

Molecules of **3** and **4** both possess C_{2v} symmetry and are identical except for the bridging atom. As expected, the Raman and IR spectra of both compounds are thus very similar. Though a normal-coordinate analysis of the vibrational modes of these compounds, as well as in **6**, is beyond the scope of this paper, many of the vibrations can be identified by comparison with other ferrocene derivatives in the literature.[32−34]

The Raman spectra of **3** and **4** are very similar between 800 and 4000 cm^{-1} (Figure 7, top). By comparison with the assignments of Raman-active modes of ferrocene and some ferrocene derivatives, tentative peak assignments have been made. Surprisingly, all of the vibrations observed in ferrocene that are attributed to Cp vibrations could be readily assigned to peaks in the Raman spectra of **3** and **4**. Three peaks near 3100 cm^{-1} are due to C−H stretching modes of the Cp rings. Though there are only two C−C stretching modes observed near 1400 cm^{-1} in ferrocene, we have assigned three peaks to C−C stretching in accord with Butler's assignments for ferrocene derivatives.[33] The C−C stretches in **3** (1349 and 1400 cm^{-1}) and **4** (1347 and 1401 cm^{-1}) are observed at lower frequency than in ferrocene (1356 and 1412 cm^{-1}).[32] Raman modes due to C−H deformations (in plane and out of plane of the Cp rings) and ring distortions are consistent with the spectrum of ferrocene. All of the peaks between 800 and 4000 cm^{-1} appear to be independent of the bridging element, indicating that they are due only to cyclopentadienyl modes.

Between 100 and 800 cm^{-1}, however, many of the Raman frequencies of **3** and **4** are significantly different, suggesting that these peaks are coupled to the pseudotetrahedral bridging element (Figure 7, bottom). Indeed, Si−C and Ge−C stretching modes are expected in this spectral region. The mode near 390 cm^{-1} has been assigned to the symmetric ring tilt of the Cp rings. It is interesting that this mode is nearly unperturbed from the same mode in ferrocene. This may reflect some torsional freedom along the Cp−E bond.

The most characteristic peak in the spectra of **3** and **4** is the symmetric ring−metal stretching mode near 300 cm^{-1}. This frequency is strongly affected by the bridging element as the peak is observed about 30 cm^{-1} higher in **3** than in **4**. The frequency of this mode has a strong dependence on the substituents of the Cp rings, as exemplified by the difference between ferrocene (306 cm^{-1}), decamethylferrocene (169 cm^{-1}), and 1,1′-dichloroferrocene (344 cm^{-1}).[34]

The Raman spectrum of **6** shows stretching vibrations due to the cyclopentadienyl rings that are consistent

(32) Long, T. V., Jr.; Huege, F. R. *Chem. Commun.* **1968**, 1239.
(33) Butler, I. S.; Harvey, P. D.; Allen, G. C. *J. Raman Spectrosc.* **1987**, *18*, 1.
(34) Phillips, L.; Lacey, A. R.; Cooper, M. K. *J. Chem. Soc., Dalton Trans.* **1988**, 1383.

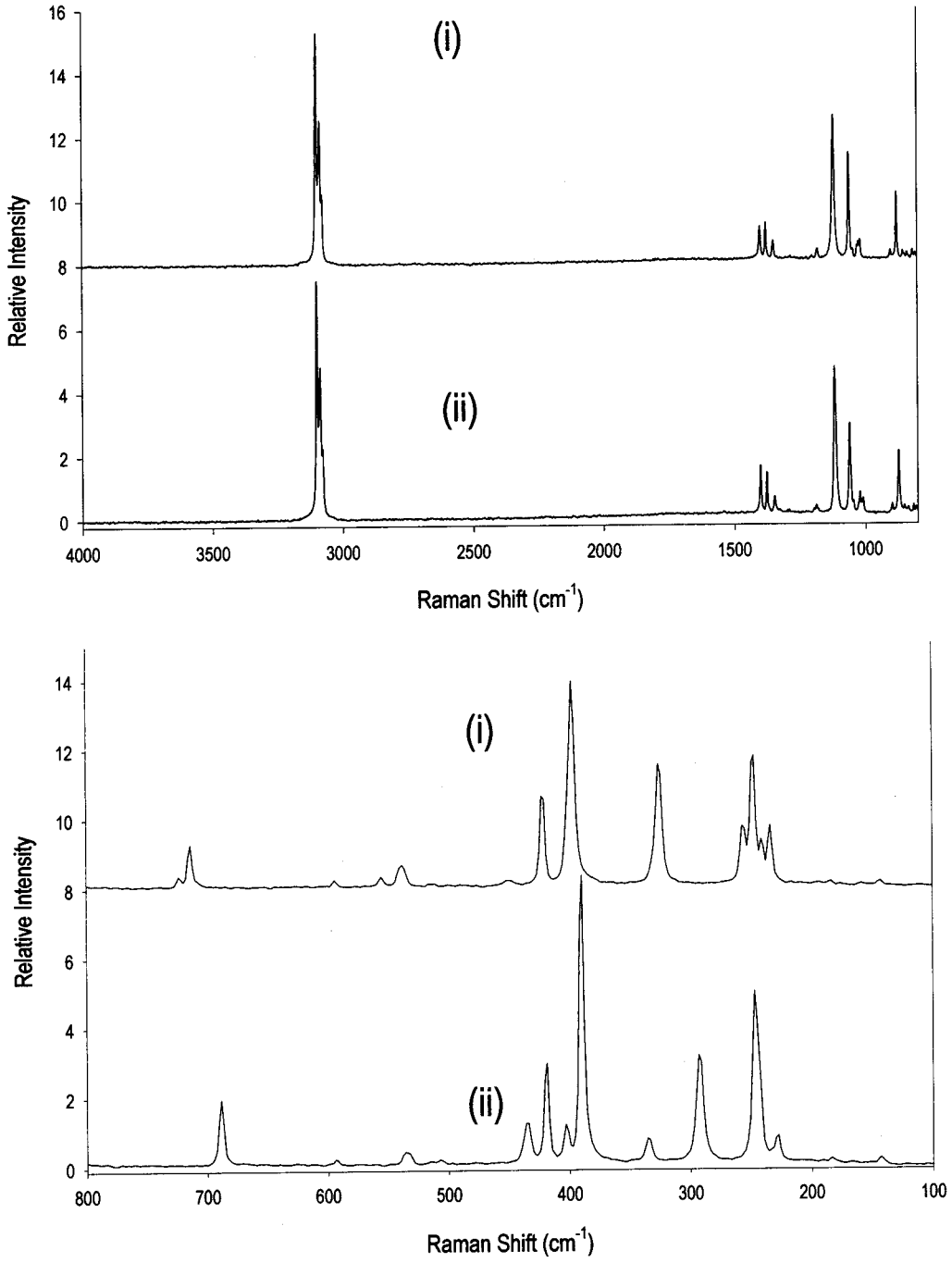

Figure 7. Raman spectra of (i) **3** and (ii) **4**. For clarity, the spectra have been divided into two regions: 4000−800 cm^{-1} (top) and 800−100 cm^{-1} (bottom).

with those of other ferrocene derivatives. Moreover, the positions of the ring stretching and deformation modes are not significantly different from those observed for **3** and **4**. The intense resonance at 316 cm^{-1} has been tentatively assigned to the Fe−Cp symmetric stretch after comparison with ferrocene and the spirocyclic [1]-ferrocenophanes.

Summary

The strained, spirocyclic [1]ferrocenophanes **3**−**5** were synthesized and characterized by a variety of techniques. Single-crystal X-ray diffraction studies revealed the presence of highly strained, ring-tilted structures. As the Fe centers in compounds **3** and **4** are in close proximity, significant metal−metal interactions were observed by cyclic voltammetry. Furthermore, Mössbauer studies of the spirocyclic [1]ferrocenophanes showed smaller quadrupolar splittings than for ferrocene. A possible interpretation of this is the presence of a metal−bridging atom interaction. Tetraferrocenylsilane **6** was prepared and structurally characterized for comparison with **3** and **4**. This compound showed four reversible one-electron oxidations by cyclic voltammetry, which were also consistent with metal−metal interactions. The first vibrational analysis of [1]ferrocenophanes was reported, and many vibrations of the ferrocenyl moiety could be assigned by analogy with the spectra of ferrocene. Detailed studies of the controlled

cross-linking of poly(ferrocenes) by spirocyclic [1]ferrocenophanes will be reported elsewhere.[12]

Experimental Section

Materials. Ferrocene, 1.6 M butyllithium in hexanes, silicon tetrachloride (semiconductor grade; 99.999%), and tetramethylethylenediamine (TMEDA) were purchased from Aldrich. Germanium tetrachloride (Strem) and cyclotrimethylenedichlorosilane (Gelest) were used as received. Dilithioferrocene·TMEDA and tributylferrocenylstannane (Fc-Sn^nBu_3) were synthesized as reported previously.[35−37]

Equipment. All reactions and manipulations were carried out under an atmosphere of prepurified nitrogen using either Schlenk techniques or an inert-atmosphere glovebox (Innovative Technologies), unless otherwise noted. Solvents were dried by standard methods, distilled, and stored under nitrogen. The 400 MHz ^{1}H NMR spectra and 100.5 MHz ^{13}C NMR spectra were recorded on a Varian Unity 400 spectrometer. The 79.5 MHz ^{29}Si NMR spectra were recorded on a Varian Unity 400 spectrometer using either a normal (for **3** and **6**) or a DEPT (for **5**) pulse sequence and were referenced externally to TMS. Room-temperature ^{57}Fe Mössbauer spectra were obtained using a Ranger Scientific Inc. VT-1200 instrument with a MS-1200 digital channel analyzer. The γ-ray source was a 6 mCi ^{57}Co sample supplied by Amersham. The data were collected in a −15.8 to +15.8 mm s^{-1} range and referenced to Fe powder. Data were acquired as long as was required to obtain a suitable fit to standard independent Lorentzian line shapes for sinusoidal baselines. Cyclic voltammograms of **3**−**5** were obtained under N_2 by analysis of ca. 5 mM dichloromethane solutions (0.1 M $[Bu_4N][PF_6]$ electrolyte) using an EG&G Princeton Applied Research Model 273 potentiostat with a Pt working electrode, a W secondary electrode, and a Ag-wire pseudo-reference electrode in a Luggin capillary. Cyclic voltammetry of **6** was performed under ambient conditions under N_2 by analysis of a 0.31 mM solution in benzonitrile using a PAR Model 173 potentiostat with a 250 μm diameter Pt disk (polished with diamond paste before use) as the working electrode and an aqueous SCE as the reference electrode, separated from the analyte solution by a fine frit. Potentials in this paper are given versus the ferrocene/ferrocenium couple. This was not used as the internal standard, however, because its wave overlapped those of the analytes. Rather, decamethylferrocene was employed as an internal standard ($E_{1/2}$ = −0.07 V versus SCE in the present experiments) and potentials were converted to the ferrocene scale by subtraction of 0.51 V for benzonitrile and 0.55 V for dichloromethane solutions. A PAR 174 potentiostat was employed for differential pulse voltammetry measurements, using a 1 s drop time and 25 mV modulation amplitude settings. UV−vis spectra were obtained in CH_2Cl_2 (ca. 5 × 10^{-4} M) on a Perkin-Elmer Lambda 900 UV−vis−near-IR spectrometer using a 1 cm quartz cuvette. IR spectra were obtained as Nujol mulls with a Nicolet Magna-IR 550 spectrometer. FT-Raman spectra were collected on a Bomems MB-157 FT-spectrometer with a Spectra Physics diode pumped Nd:YLF laser (1064 nm; 350 kHz repetition rate). The instrument was configured in 180° backscattering mode using sealed glass capillary tubes to hold the neat, crystalline samples. Electron impact (EI) mass spectra were obtained with a VG 70-250S mass spectrometer. Elemental analyses were performed by Quantitative Technologies Inc., Whitehouse, NJ.

Synthesis of the Spirocyclic [1]Silaferrocenophane 3. This compound was synthesized in the same manner as was used by Osborne, but with modifications to the workup which we found to improve the yield substantially.

Tetrachlorosilane (0.65 mL, 5.7 mmol) was added slowly via syringe to a suspension of dilithioferrocene·TMEDA (4.47 g, 14.2 mmol) in 100 mL of hexanes cooled to −78 °C. The solution was then warmed slowly to room temperature over a period of 3 h, giving a deep red solution with an orange precipitate. The reaction mixture was then heated to reflux for 3 h. After the solution was cooled to room temperature with a water bath, 0.5 mL of *n*-butanol was added to quench the excess dilithioferrocene and the mixture was stirred for 10 min. The solution was cooled to −10 °C and filtered on a Buchner funnel. The orange residue was dissolved in dichloromethane to give a cloudy, red solution. Following filtration through a Buchner funnel and a 10 cm column (5 cm diameter) of alumina (BDH, Brockman, activity II; 100−200 mesh) under air, the solution was rotary-evaporated to dryness. The solid was redissolved in a minimum of dichloromethane and was chromatographed on a 30 cm × 5 cm column of alumina (hexanes), and the initial yellow band (ferrocene) was discarded. Compound **3** eluted with dichloromethane and was rotary-evaporated to dryness, affording 1.57 g (4.0 mmol, 70%) of **3**. Compound **3** is obtained as red, air-stable crystals moderately soluble in toluene, benzene, THF, dichloromethane, and chloroform and nearly insoluble in hexanes and DMSO.

Data for 3: ^{13}C NMR (100.5 MHz, C_6D_6) δ 78.3 (Cp), 75.5 (Cp), 31.1 (*ipso*-Cp) ppm; ^{1}H NMR (400 MHz, C_6D_6) δ 4.47 (s, 16H, Cp) ppm; ^{29}Si NMR (79.5 MHz, C_6D_6) δ −16.6 ppm. MS (EI, 70 eV) *m*/*z* (%) 396 (M^+, 100); Mössbauer spectrum doublet, IS = 0.44, QS = 2.01 mm s^{-1}; UV−vis (CH_2Cl_2) λ (ϵ) 483 (590) nm (L mol^{-1} cm^{-1}); IR (Nujol mull) 1178, 1122, 1032, 1019, 1013, 890, 881, 852, 803 (d), 696, 567, 536, 509 cm^{-1}.

Synthesis of the Spirocyclic [1]Germaferrocenophane 4. This compound was synthesized in the same manner as was used by Osborne and co-workers, but a modified workup procedure afforded a measurable yield. Germanium tetrachloride (0.75 mL, 6.6 mmol) was added dropwise via syringe to a stirred suspension of dilithioferrocene·TMEDA (4.92 g, 15.7 mmol) in 100 mL of hexanes at −78 °C. The solution was warmed to room temperature over 3 h. After the reaction mixture was refluxed for 10 min, the hot mixture was gravity-filtered under air. The filtrate was rotary evaporated to dryness, giving an orange-red crystalline solid. Once redissolved in dichloromethane, the clear, red solution of **4** was flash-chromatographed through a 10 cm × 5 cm column of alumina (BDH, Brockman, activity II; 100−200 mesh). The red solution was rotary-evaporated to dryness to give red crystals which were ca. 95% pure by NMR, with ferrocene as the major impurity. Recrystallization from dichloromethane afforded ca. 100−150 mg (0.23−0.34 mmol, 3−5%) of red, air-stable crystals. Variation of reaction conditions including longer reflux times, lower reaction temperature, different solvents (THF, ether) and stoichiometries, and alternative workup procedures (e.g. omission of the flash chromatography) gave no improvement in the yield.

Data for 4: ^{13}C NMR (100.5 MHz, C_6D_6) δ 77.7 (Cp), 76.0 (Cp), 27.8 (*ipso*-Cp) ppm; ^{1}H NMR (400 MHz, C_6D_6) δ 4.46 (t, 8H, Cp), 4.40 (t, 8H, Cp) ppm; MS (EI, 70 eV) *m*/*z* (%) 442 (M^+, 100), 368 (M^+ − Ge, 92); Mössbauer spectrum doublet, IS = 0.45, QS = 2.09 mm s^{-1}; UV−vis (CH_2Cl_2) λ (ϵ) 489 (560) nm (L mol^{-1} cm^{-1}); IR (Nujol mull) 1294, 1183, 1117, 1024, 876, 848, 804, 662, 532, 514 cm^{-1}.

Synthesis of Spirocyclic [1]Silaferrocenophane 5. Cyclotrimethylenedichlorosilane (3.0 mL, 26 mmol) was added dropwise to a stirred suspension of 5.31 g (16.9 mmol) of dilithioferrocene·TMEDA in 100 mL of diethyl ether cooled to −78 °C. The solution was warmed slowly to 0 °C over a period of 2 h. At −60 °C the solution started to turn red and was deep red at −40 °C. The reaction mixture was filtered through a frit at 0 °C to give a deep red, clear solution. The ether was removed under vacuum to leave dark red crystals. After

(35) Rausch, M. D.; Ciappenelli, D. J. *J. Organomet. Chem.* **1967**, *10*, 5025.
(36) Guillaneux, D.; Kagan, H. B. *J. Org. Chem.* **1995**, *60*, 2502.
(37) Bishop, J. J.; Davison, A.; Katcher, M. L.; Lichtenberg, R. E.; Merrill, J. C.; Smart, J. *Organomet. Chem.* **1971**, *27*, 241.

drying under dynamic vacuum at room temperature for 24 h, the product was dissolved in a minimum volume of hexanes and filtered again. Recrystallization at low temperature gave large red needles. Subsequent sublimation at 40 °C afforded 3.39 g (13.3 mmol, 79%) of pure **5**. These deep red crystals possess a pungent odor and are very air- and moisture-sensitive. Compound **5** is very soluble in toluene, hexanes, THF, benzene, and dichloromethane.

Data for 5: ^{13}C NMR (100.5 MHz, C_6D_6) δ 78.0 (Cp), 74.7 (Cp), 31.9 (*ipso*-Cp), 18.3 ($CH_2CH_2CH_2$), 16.0 ($SiCH_2$) ppm; ^{1}H NMR (400 MHz, C_6D_6) δ 4.39 (s, 4H, Cp), 4.04 (s, 4H, Cp), 2.38 (qt, $^3J_{HH}$ = 8.2 Hz, 2H, $CH_2CH_2CH_2$), 1.44 (t, $^3J_{HH}$ = 8.2 Hz, 4H, $SiCH_2$) ppm; ^{29}Si NMR (79.5 MHz, C_6D_6) δ 3.6 ppm; MS (EI, 70 eV) *m*/*z* (%) 254 (M^+, 100), 226 ($M^+ - C_2H_4$, 62), 213 ($M^+ - C_3H_5$, 20), 148 ($(C_5H_4)FeSi^+$, 38); UV−vis (CH_2Cl_2) λ (ϵ) 482 (420) nm (L mol^{-1} cm^{-1}); mp 92 °C. Anal. Calcd for $C_{13}H_{14}FeSi$: C, 61.43; H, 5.55. Found: C, 61.29; H, 5.40.

Synthesis of Tetraferrocenylsilane 6. This compound was prepared by the patented procedure of Rosenberg. A solution of 20.25 g of $FcSn^nBu_3$ (42.6 mmol) dissolved in 125 mL of THF was cooled to −78 °C in a dry ice/acetone bath. With stirring, 26 mL of 1.56 M ^{n}BuLi (in pentanes; 40.6 mmol) was added via syringe to give an orange-red solution. After 2 h of stirring at −78 °C, 1.0 mL of $SiCl_4$ (1.5 g, 8.7 mmol) was added and the solution was slowly warmed to room temperature. The reaction mixture was then refluxed for 16 h at 70 °C. The solvent was reduced to ca. 40 mL under vacuum, giving an orange precipitate and a red liquid. Ethanol (95%, 125 mL) was added to the flask, and the solution was warmed to 50 °C with constant stirring. After it was cooled to −55 °C in a freezer, the crude product was isolated on a Buchner funnel and washed with 3 × 20 mL of cold ethanol; the filtered solution was discarded. The solid was dissolved in a minimum of CH_2Cl_2 and filtered twice through a short (ca. 15 cm) column of alumina. Rotary evaporation afforded 4.15 g of an orange-yellow solid. Recrystallization from CH_2Cl_2/hexanes (ca. 2:1) afforded 2.34 g (3.05 mmol, 35%) of orange-red needles.

Data for 6: ^{13}C NMR (100.5 MHz, C_6D_6) δ 74.3 (Cp), 71.5 (*ipso*-Cp), 70.7 (Cp), 69.2 (Cp) ppm; ^{1}H NMR (400 MHz, C_6D_6) δ 4.46 (t, $^3J_{HH}$ = 1.76 Hz, 8H, Cp), 4.30 (t, $^3J_{HH}$ = 1.71 Hz, 8H, Cp), 4.02 (s, 20H, Cp) ppm; ^{29}Si NMR (79.5 MHz, CD_2Cl_2) δ −10.1 ppm; MS (EI, 70 eV) *m*/*z* (%) 768 (M^+, 100), 517 ($M^+ - Fc - C_5H_5$, 49); Mössbauer spectrum doublet, IS 0.43, QS = 2.26 mm s^{-1}; UV−vis (CH_2Cl_2) λ (ϵ) 452 (490) nm (L mol^{-1} cm^{-1}).

X-ray Structure Determination Technique. Crystals of **3**−**6** were each mounted on a glass fiber and coated with epoxy glue. The orange-red prisms of **3** and **4** had dimensions of approximately 0.3 × 0.3 × 0.1 mm and 0.2 × 0.2 × 0.05 mm, respectively. Due to surface decomposition (hydrolysis), the dimensions of the crystal of **5** could not be measured (all were less than 0.5 mm). The crystal of **6** was an orange needle with approximate dimensions of 0.31 × 0.15 × 0.15 mm. Intensity data for the compounds **3**−**6** were collected at 168(2) K on a Siemens P4 diffractometer using graphite-monochromated Mo Kα radiation (λ = 0.710 73 Å). The ω-scan technique was applied with variable scan speeds. Intensities of 3 standard reflections were measured every 100 reflections; all four crystals showed negligible decay (<1%) during the data collection. A semiempirical absorption correction was applied using the SHELXA-90 routine in SHELXL.[38]

The positions of all atoms for **3**, **5**, and **6** were determined by direct methods using Siemens SHELXTL PC.[39] For each structure, all non-hydrogen atoms were refined anisotropically by full-matrix least squares to minimize $\Sigma w(F_o^2 - F_c^2)^2$, where $w = 1/[\sigma^2(F_o)^2 + (aP)^2]$, $P = (\mathrm{Max}(F_o^2,0) + 2F_c^2)/3$, and a is the weighting factor listed in Table 1. The structure of **4** was solved using the solution of **3** and refined in a similar manner. For compounds **3**−**6** the hydrogen atoms were refined isotropically. Crystal data, details of data collection, and least-squares parameters are listed in Table 1. Selected bond lengths and bond angles are provided in Tables 2, 3, 5, and 6. All calculations were performed and all diagrams (Figures 1−4) were created using SHELXTL-PC and SHELXL-93 on a 486 personal computer.

Acknowledgment. M.J.M. thanks the Natural Sciences and Engineering Research Council of Canada (NSERC) for a Postgraduate Scholarship (1995−1999). I.M. thanks the Alfred P. Sloan Foundation for a Research Fellowship (1994−1998), the NSERC for an E.W.R. Steacie Fellowship (1997−1999), and the University of Toronto for a McLean Fellowship (1997−2003).

Supporting Information Available: Tables of all bond lengths and angles, anisotropic thermal parameters, and atomic coordinates (37 pages). Ordering information is given on any current masthead page.

OM971071I

(38) Sheldrick, G. M. SHELXA 90: Program for absorption correction; University of Göttingen, Göttingen, Germany, 1990.

(39) Sheldrick, G. M. SHELXTL-PC; Siemens Analytical X-ray Instruments Inc., Madison, WI, 1994.